JOURNAL OF VIROLOGY, Feb. 2010, p. 2100–2109 Vol. 84, No. 4
0022-538X/10/$12.00 doi:10.1128/JVI.01557-09

Dynamin- and Clathrin-Dependent Endocytosis in African Swine Fever Virus Entry[▽]

Bruno Hernaez and Covadonga Alonso*

Departamento de Biotecnologia-Instituto Nacional de Investigacion y Tecnologia Agraria y Alimentaria, INIA, Autovia A6 km 7, 28040 Madrid, Spain

Received 28 July 2009/Accepted 13 November 2009

African swine fever virus (ASFV) is a large DNA virus that enters host cells after receptor-mediated endocytosis and depends on acidic cellular compartments for productive infection. The exact cellular mechanism, however, is largely unknown. In order to dissect ASFV entry, we have analyzed the major endocytic routes using specific inhibitors and dominant negative mutants and analyzed the consequences for ASFV entry into host cells. Our results indicate that ASFV entry into host cells takes place by clathrin-mediated endocytosis which requires dynamin GTPase activity. Also, the clathrin-coated pit component Eps15 was identified as a relevant cellular factor during infection. The presence of cholesterol in cellular membranes, but not lipid rafts or caveolae, was found to be essential for a productive ASFV infection. In contrast, inhibitors of the Na^+/H^+ ion channels and actin polymerization inhibition did not significantly modify ASFV infection, suggesting that macropinocytosis does not represent the main entry route for ASFV. These results suggest a dynamin-dependent and clathrin-mediated endocytic pathway of ASFV entry for the cell types and viral strains analyzed.

Many animal viruses have evolved to exploit endocytosis to gain entry into host cells after initial attachment of virions to specific cell surface receptors. To date, a number of different routes of endocytosis used by viruses have been characterized, including clathrin-mediated endocytosis, uptake via caveolae/lipid rafts, macropinocytosis, phagocytosis, and other routes that are currently poorly understood.

In recent years, viruses have also been used as tools to study cellular endocytosis and membrane trafficking at the molecular level, with there being special interest in the regulation of the diverse routes (31), since examples of viruses using each route can be found (reviewed in references 26, 31, and 38). The clathrin-mediated endocytic route has been the most extensively studied at the molecular level, and it has been shown to be used by diverse mammalian enveloped viruses, such as vesicular stomatitis virus (42), Semliki Forest virus (19), and West Nile virus (11), to infect cells. Influenza virus and HIV-1 also can use this pathway as an alternative route of entry (12, 39). Clathrin is assembled on the inside face of the plasma membrane to form a characteristic coated pit (CCP). During this process, clathrin also interacts with a number of essential molecules, including Eps15, adapter protein AP2, and dynamin GTPase (9). Additionally, clathrin-mediated endocytosis also provides endocytic vesicles as an acidified environment for those viruses that require a low-pH step during the first stages of infection to initiate capsid destabilization and genome uncoating. On the other hand, the lipid raft/caveola-based route is generally used by those acid-independent viruses. Recently, macropinocytosis is generating growing interest, since it has been demonstrated to be induced by some viruses from diverse families, such as vaccinia virus and adenovirus serotype 3 (5, 29), to gain entry into cells.

In this study, we have focused on the entry of African swine fever virus (ASFV), a large enveloped DNA virus with a genomic composition similar to that of poxviruses, although the virion structure and morphology resemble those of iridoviruses. At present, it is the sole member of the newly created family *Asfarvirida*e (16, 43). It is the etiologic agent responsible for a highly lethal and hemorrhagic disease affecting domestic swine, which often results in important economic losses in affected countries because of the high rate of mortality associated with this illness and the lack of an effective vaccine.

Early studies of the entry of BA71V, a Vero cell-adapted ASFV strain, into host cells showed that this internalization of virus particles is a temperature-, energy-, and low-pH-dependent process, since it does not occur at 4°C or in the presence of inhibitors of cellular respiration or lysosomotropic agents (2, 44). All these features are consistent with a receptor-mediated endocytosis mechanism of entry. However, there are still numerous questions to be answered. One of them is the nature of the cellular receptor(s) that mediates ASFV entry, which remains largely unknown, although a correlation between cell susceptibility to infection and expression of porcine CD163 on the surface of swine monocytes/macrophages has been reported (36). In regard to the viral components involved in this initial step, the p12 and p54 proteins were shown to play a role during attachment to the cell surface and p30 during internalization, as inferred from previous studies with neutralizing antibodies against p30 and p54 (17) and blockage of infection after saturation of virus binding sites with recombinant p12 (6). Early electron microscopy (EM) studies (2, 45) revealed that attachment of ASFV virions to the cell surface often occurs in coated pits; however, their later presence inside coated vesicles is not fully clear. After attachment, virions are detected inside

* Corresponding author. Mailing address: Departamento de Biotecnologia-Instituto Nacional de Investigacion y Tecnologia Agraria y Alimentaria, INIA, Autovia A6 km 7, 28040 Madrid, Spain. Phone: 34-91-3476896. Fax: 34-91-3478771. E-mail: calonso@inia.es.

[▽] Published ahead of print on 25 November 2009.

endosomes, where fusion with the viral membrane takes place. The ASFV cycle continues with the transport of viral cores via retrograde transport along microtubules to reach a perinuclear area, known as the viral factory, where replication occurs (4).

In recent times, knowledge about different endocytic pathways and their regulatory molecules has notably increased, and the development of molecular tools to study these processes is becoming increasingly precise (38). In the present study, we examined the ASFV infection using a variety of chemical inhibitors and dominant negative molecules to disrupt different endocytic pathways. Our results confirmed a major role for dynamin-dependent and clathrin-mediated endocytosis during the first stages of ASFV infection, with no significant differences in the behavior of the two ASFV strains and the two cell lines analyzed.

MATERIALS AND METHODS

Cells, viruses, and infections. Vero cells were grown at 37°C in a 5% CO_2 atmosphere in Dulbecco's modified Eagle's medium (DMEM) supplemented with 5% fetal bovine serum (FBS). WSL-R line 379 is a macrophage cell line from wild swine origin that was kindly provided by Günther Kiel (Friedrich-Loeffler Institut, Greifswald, Germany) and grown in Iscove's medium (Gibco) plus F-12 nutrient mixture (Gibco) plus 10% FBS. The BA71V (adapted to grow in Vero cells) and 608 VR13 (with a low number of passages in Vero cells [3]) ASFV isolates were used in infection experiments carried out at 37°C with 5% CO_2. In most cases, ASFV stocks from culture supernatants were clarified and semipurified from vesicles by ultracentrifugation at 40,000 × *g* through a 40% (wt/vol) sucrose cushion in phosphate-buffered saline (PBS) for 1 h at 4°C. Virus stocks or infective ASFV yields from samples infected after drug treatment were titrated by plaque assay in Vero cells as previously described (22). Briefly, preconfluent monolayers of Vero cells in six-well plates were inoculated with 10-fold serial dilutions from samples for 90 min at 37°C. the inoculum was then removed and 3 ml of semisolid medium added (1:1 low-melting-point agarose [Gibco] and 2× minimal essential medium [MEM] [Lonza]). Correct plaque development took 10 to 12 days, and visualization was possible after staining with crystal violet (Sigma). After viral inoculum addition, when synchronization of infection was required, virus adsorption was performed for 90 min at 4°C, and after cold washing, cells were rapidly shifted to 37°C.

Vectors encoding dominant negative mutants. Vectors encoding green fluorescent protein (GFP)-Eps15 and a corresponding dominant negative mutant version (GFP-EΔ95/295) were kindly provided by A. Dautry-Varsat (Institut Pasteur). Vectors encoding dynamin-GFP and dominant negative mutant dynamin-K44A-GFP were kindly provided by S. L. Schmid (The Scripps Research Institute). pEGFP-N1 was purchased from Clontech and was used as a control.

Transfections were performed by using the Fugene 6 transfection reagent from Roche as specified by the manufacturer. Briefly, Vero cells were grown on glass coverslips in 24-well tissue culture plates, in the absence of antibiotics, until 80% confluence, and then 400 ng DNA was mixed with 3 μl Fugene 6 and incubated for 40 min at room temperature before addition to cells. To minimize cytotoxicity, after 5 h the transfection mixture was removed from cells and fresh medium added. At 24 h after transfection, cells were infected with ASFV isolates (1 PFU/cell), and infected cells were detected and analyzed by immunofluorescence at 6 h postinfection (hpi).

Transferrin (TF), dextran (DXT), and cholera toxin (CTX) uptake assays. Cells, grown on glass coverslips to 60% confluence, were serum starved for 30 min prior to incubation with 50 μg/ml Alexa Fluor 594-labeled human transferrin (Molecular Probes) in DMEM for 20 min at 4°C for binding. Cells were then cold washed with DMEM and transferred to 37°C for 15 min. Residual and noninternalized labeled TF was removed by acid washing with 0.1 M NaCl–0.1 M glycine, pH 3.0. Cells were then processed for immunofluorescence and examined by confocal microscopy.

Likewise, dextran uptake assays were performed using Alexa Fluor-594 labeled 10,000-molecular-weight (MW) dextran (Molecular Probes). Starved cells were incubated with 0.5 mg/ml labeled dextran for 10 min at 37°C. DXT uptake was stopped by washing three times with ice-cold PBS, and surface-bound DXT was washed off in cold 0.1 M sodium acetate–0.05 M NaCl (pH 5.5) for 10 min.

Cholera toxin subunit B from *Vibrio cholerae* labeled with Alexa Fluor A488 (Molecular Probes) was diluted to 1 μg/ml in DMEM–2% FBS, added to cells, and left for 15 min at 4°C followed by additional 10 min at 37°C. Cells were then rapidly cold washed in PBS three times, processed for immunofluorescence, and examined by confocal microscopy.

Indirect immunofluorescence and confocal microscopy. Vero cells growing on glass coverslips were fixed in PBS–3.8% paraformaldehyde for 10 min and permeabilized with PBS–0.1% Triton X-100 for 12 min. Following fixation, aldehyde fluorescence was quenched by incubation of cells with 50 mM NH_4Cl in PBS for 15 min. Working dilutions of the primary antibodies used were 1:100 for monoclonal antibody against clathrin heavy chain (BD Sciences), 1:100 for monoclonal antibody against ASFV protein p30, and 1:500 for rabbit serum raised against ASFV structural protein pE120R. The secondary antibodies used (Molecular Probes) were anti-mouse immunoglobulin G (IgG) antibody conjugated to Alexa Fluor 488 or Alexa Fluor 594 and anti-rabbit IgG antibody conjugated to Alexa Fluor 594. All secondary antibodies were purchased from Molecular Probes and diluted 1:200. Specificity of labeling and absence of signal crossover were determined by examination of single labeled control samples.

Confocal microscopy was carried out in a Leica TCS SPE confocal microscope using a 63× objective, and image analyses were performed with Leica Application Suite advanced fluorescence software (LAS AF).

Drug treatments and FACS analyses. Stock solutions of inhibitors were prepared as follows: 10 mM dynasore (Calbiochem), 0.5 mM latrunculin A (Calbiochem), 0.5 mM jasplakinolide (Calbiochem), 5 mM nystatin (Sigma), and 50 mM 5-ethylisopropyl amiloride (EIPA; Sigma) stock solutions were all prepared in dimethyl sulfoxide (DMSO), while 20 mM chlorpromazine (CPZ) (Sigma), 100 mM chloroquine (Sigma), 150 μM bafilomycin A1 (Sigma), and 25 mM methyl-β-cyclodextrin (CD) (Sigma) were prepared in water. We first ensured that cell death, determined by the trypan blue exclusion method, did not exceed 10% after incubation of cell cultures with different inhibitors at the indicated working concentrations. Cells were pretreated for 30 min with inhibitors at the indicated concentrations in growth medium for 30 min at 37°C, followed by cold synchronized infections with ≤1 PFU of ASFV isolate per cell. Where indicated, chlorpromazine was added to previously infected cells at 3 hpi. All inhibitors (except methyl-β-cyclodextrin, which was removed from cells at 2 hpi) were present throughout all the experiment, and at 6 hpi cells were washed with PBS and harvested by trypsinization. After washing with fluorescence-activated cell sorter (FACS) buffer (PBS, 0.01% sodium azide, and 0.1% bovine serum albumin [BSA]), cells were fixed and permeabilized with Perm2 (BD Sciences) for 10 min at room temperature. Detection of infected cells was performed by incubation with anti-p30 monoclonal antibody (diluted 1:100 in FACS buffer) for 30 min at 4°C, followed by incubation with phycoerythrin (PE)-conjugated anti-mouse immunoglobulins (1:50, diluted in FACS buffer [Dako]) for 30 min at 4°C. After extensive washing, 2×10^4 cells per time point were scored and analyzed in a FACSCalibur flow cytometer (BD Sciences) to determine the percentage of infected cells under these conditions. Determination of control infection rates under these conditions yielded 25 to 30% of total cells examined. Infection rates obtained after drug treatments were normalized to infected cell percentages found in control plates. Mean values from at least three experiments were statistically compared to values obtained for control cells (untreated and infected) using two-tailed Student *t* tests with a confidence level of 95%, and significant differences are indicated by asterisks in the figures.

Cholesterol determination. Cell extracts from approximately 10^5 Vero cells were prepared in 0.1 M mM Tris (pH 8.0), 100 mM NaCl, 1% NP-40, and 2 mM $CaCl_2$. The levels of cholesterol from these cell extracts were measured with the Amplex Red cholesterol assay kit (Molecular Probes) following the manufacturer's instructions. Twenty-five-microliter portions of cell extracts and cholesterol standards were incubated with 25 μl of Amplex Red working solution for 30 min at 37°C, protected from light, in 96-well plates. Fluorescence at 590 nm was subsequently measured in a Genios Spectrafluor microplate reader (Tecan).

Western blotting. Cells seeded in 24-well plates were harvested and lysed on ice in 80 μl lysis buffer (150 mM NaCl, 5 mM β-mercaptoethanol, 1% NP-40, 0.1% SDS, 50 mM Tris [pH 8.0]) containing protease inhibitors (complete EDTA-free protease inhibitors; 1 tablet/10 ml of buffer [Roche Molecular Biochemicals]) per well. After 20 min on ice, cell extracts were clarified by centrifugation at 4°C for 15 min at 17,000 × *g*. After estimation of total protein in samples by the Bradford method, equal amounts of protein mixed with Laemmli sample buffer were electrophoresed and transferred onto nitrocellulose membranes (Bio-Rad). To detect protein p30 and β-actin (as a protein loading control), membranes were incubated with a anti-p30 monoclonal antibody diluted 1:500 as previously described (21) and a rabbit polyclonal antibody (Sigma) diluted 1:500. The horseradish peroxidase (HRP)-coupled secondary antibodies used were anti-mouse (GE Healthcare) or anti-rabbit (GE Healthcare) antibodies diluted 1:5,000. Bands obtained after development with ECL reagent (GE Healthcare) and corresponding to p30 and β-actin were densitometrically quan-

tified, and data were normalized to control values using an image analyzer with the TINA software package (Raytest).

RESULTS

Infection by ASFV is dependent on cellular dynamin. Dynamin is a 100-kDa GTPase which plays an essential role in cellular membrane fission during vesicle formation and therefore is required for clathrin- and caveola-mediated endocytosis but not for macropinocytosis (13, 20, 37). To ascertain whether ASFV infection is dynamin dependent or not, we explored the effect of the dynamin dominant negative mutant Dyn-K44A, which was previously described to have decreased GTPase activity resulting in reduced endocytosis (14). We first analyzed, by confocal laser scanning microscopy, the ability of the K44A mutant to inhibit endocytosis in Vero cells by examining internalization of labeled transferrin (TF-A_{594}), which is typically mediated by clathrin-mediated endocytosis. As described for other cell types, in 85 to 90% of Vero cells the transient overexpression of Dyn-K44A (24 h after transfection) nearly abolished the internalization of TF-A_{594}. Nevertheless, in those control cells expressing either GFP or wild-type dynamin (Dyn-WT), normal endocytosis was observed, as indicated by punctate staining in the perinuclear region (Fig. 1A). Likewise, at 24 h after transient transfection, Vero cells expressing GFP, Dyn-WT, or Dyn-K44A were infected with BA71V (1 PFU/cell) and infection was allowed to proceed until 6 hpi, when expression of ASFV early protein p30 is detectable with specific monoclonal antibodies. As shown in Fig. 1B and C, ASFV infection was significantly reduced in cells transfected with the dynamin mutant K44A vector compared to cells transfected with wild-type dynamin or GFP vectors. In fact, most of those cells transfected with Dyn-K44A that also were infected were expressing low levels of Dyn-K44, as judged by GFP fluorescence intensity. These low expression levels of the Dyn-K44A mutant were also correlated with residual TF-A_{594} internalization, indicating that endocytosis was not completely inhibited in those cells (data not shown). This result suggests that a complete inhibition of endocytosis is required to prevent ASFV infection.

To further confirm these results, dynasore (25), a specific inhibitor of the GTPase activity of dynamin that blocks the internalization of labeled TF, was used. We preincubated Vero cells with different concentrations of dynasore for 30 min prior to BA71V infection (multiplicity of infection [MOI] of <1 PFU/cell, to avoid unspecific viral uptake) and scored infected cells at 6 hpi by FACS. Infection of cells as detected by viral protein p30 expression provides a clear quantitative end point assay, and the infection rates obtained for untreated cells at the low MOI used were around 25 to 30%. The inhibitor caused a 10-fold, dose-dependent drop in ASFV infectivity (Fig. 2A). An even more pronounced inhibition of infectivity caused by a lower dynasore dose was observed in WSL cells, suggesting similar behavior for ASFV in different cell lines. This reduction in ASFV infectivity correlated with a reduction of the expression of early viral protein p30 (Fig. 2B) detected by Western blotting of Vero infected cell extracts. Compared to that in untreated cells, the amount of p30 protein at 6 hpi was reduced to 34% in a dose-dependent fashion in dynasore-treated cells. Together, these results strongly suggest that ASFV entry into cells for effective infection (meaning positive early viral protein expression after virus entry) is dynamin dependent.

Relevance of clathrin-mediated endocytosis and Eps15 during ASFV infection. ASFV infection depends on endosomal acidification (and is therefore sensitive to lysosomotropic drugs) (45) and also on dynamin GTPase activity, which are hallmarks of clathrin-mediated endocytosis. Also, previous observations by EM showed that ASFV virions were often adsorbed to cytoplasmic invaginations similar to the clathrin-coated pits (2). To confirm those results, we infected monolayers of Vero cells with purified BA71V virions (MOI of >10 PFU/cell) at 4°C for 1 h and rapidly shifted them to 37°C. Cells were then fixed at increasing times (0 to 20 min after adsorption) and stained with specific antibodies against ASFV structural protein pE120R and the clathrin heavy chain. Confocal microscopy studies revealed that about 60% of virions colocalized with clathrin during the period of time examined at the first stages of infection (Fig. 3A).

Then, to assess the functional role of clathrin-mediated endocytosis in ASFV entry, we examined the inhibitory effect of chlorpromazine (CPZ). Chlorpromazine is known to prevent assembly of coated pits at the plasma membrane and causes clathrin lattices to assemble on endosomal membranes (38). Treatment of Vero cells with 5 μM CPZ significantly reduced labeled TF internalization, which takes place by clathrin-based endocytosis, and up to 14 μM completely abolished TF uptake (Fig. 3B). Higher CPZ concentrations resulted in cell detachment. This inhibition of endocytosis correlated with a reduction of ASFV infectivity in a dose-dependent manner. First, the drug was added 30 min before infection. With 2 μM chlorpromazine BA71V-infected cells were reduced to 60%, and with 14 μM they were reduced to fewer than 10% (Fig. 4A), similar to reductions in the number of infected cells after treatment with the lysosomotropic drugs chloroquine and bafilomycin A1. A similar inhibition of infection by chlorpromazine was achieved in treated WSL cells (Fig. 4A), and also no significant differences in the percentages of infected cells were found when these were infected with the 608 VR13 ASFV strain (only 13 passages in Vero cells) compared to BA71V after CPZ treatment (Fig. 4B), indicating a similar and cell type-independent clathrin requirement for both ASFV isolates tested. In contrast, when CPZ was added later in infection (at 3 hpi), after ASFV entry, no significant modification of the number of infected cells was observed. This result indicates the involvement of clathrin-mediated endocytosis during ASFV internalization but not between 3 and 6 hpi.

We next examined the effect of chlorpromazine on virus titers obtained from cell cultures 24 h after infection at a low MOI. As expected, the reduction found in BA71V infectivity after CPZ treatment correlated with a dose-dependent decrease in viral titers, with a maximum reduction of 2 log units at 14 μM CPZ. This reduction in viral titers was similar to that obtained after inhibition of endosome acidification with lysosomotropic drugs (Fig. 4C). Similar results were obtained with the 608 VR13 ASFV isolate (data not shown). Likewise, expression levels of viral protein p30, detected by Western blotting from infected cell cultures, also were diminished after chlorpromazine inhibition. This reduction was equivalent to that found after arrest of endosome acidification by chloroquine or bafilomycin A. To verify that the lower levels of p30

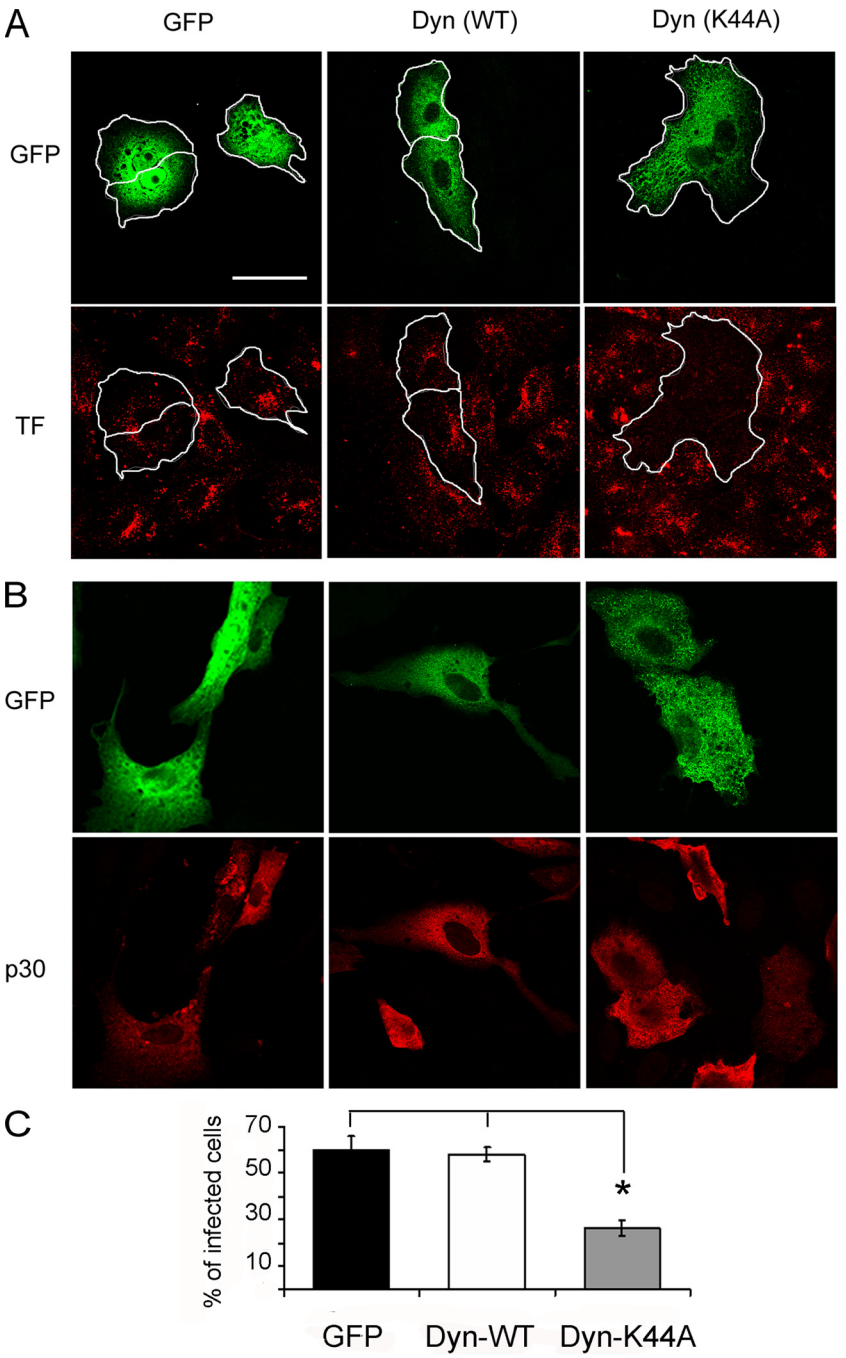

FIG. 1. Inhibition of ASFV infection by transient expression of dynamin dominant negative mutant K44A. Vero cells were transfected with GFP, wild-type dynamin-GFP, and K44A-GFP plasmids. (A) At 24 h after transfection, cells were examined by confocal microscopy for TF-A_{594} uptake. Bar, 30 μm. (B) Likewise, transfected cells were infected with BA71V, and infected cells at 6 hpi were detected as those positive for immunofluorescence with anti-p30 monoclonal antibody followed by anti-mouse Alexa 594-conjugated secondary antibody. (C) Percentages of transfected and infected cells. More than 100 transfected cells were examined in each case, and the means and standard deviations correspond to three independent experiments (asterisk, $P < 0.05$).

observed by Western blotting resulted from an inhibition of the infection by chlorpromazine and not from a reduced expression of ASFV proteins, infected cells were analyzed by immunofluorescence microscopy. Expression levels of p30 in individual cells appeared to be similar in chlorpromazine-treated cells and in control cells (Fig. 4D and data not shown).

The use of chlorpromazine and other drugs to examine viral endocytosis pathways has been well documented. However, we further confirmed the role of clathrin-mediated endocytosis in ASFV infection using a more precisely targeted inhibitor. We used the dominant negative mutant of Eps15, a protein that binds to the AP-2 adapter and is required for internalization

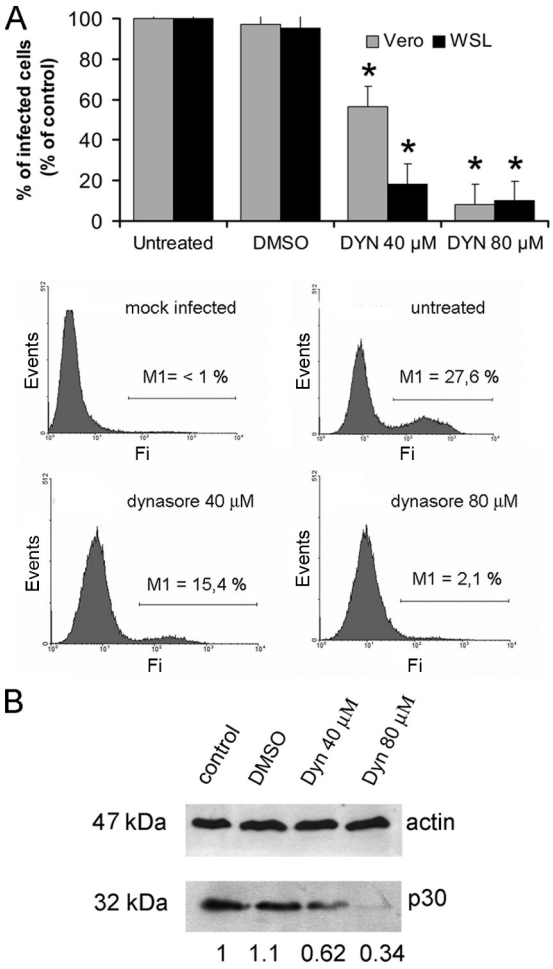

FIG. 2. ASFV infection is sensitive to dynamin inhibition by dynasore. (A) Vero and WSL cells were pretreated with different concentrations of dynasore and then infected with BA71V for 6 h. Infected cells were detected by FACS and data normalized to infection rates in untreated cells. Error bars indicate standard deviations from three independent experiments. Representative FACS profiles (events versus fluorescence intensity [Fi]) obtained during the analysis are shown below the graphs. Infected cells were gated in M1 and expressed as a percentage of total cell analyzed. (B) As previously, Vero cells were incubated with dynasore and then infected with BA71V. Cells were lysed at 6 hpi, and p30 expression was monitored by Western blotting. β-Actin was detected as control for protein loading. Results are from a representative experiment of three independent experiments performed. Quantification of the bands corresponding to p30 was corrected with β-actin data and then normalized to control values.

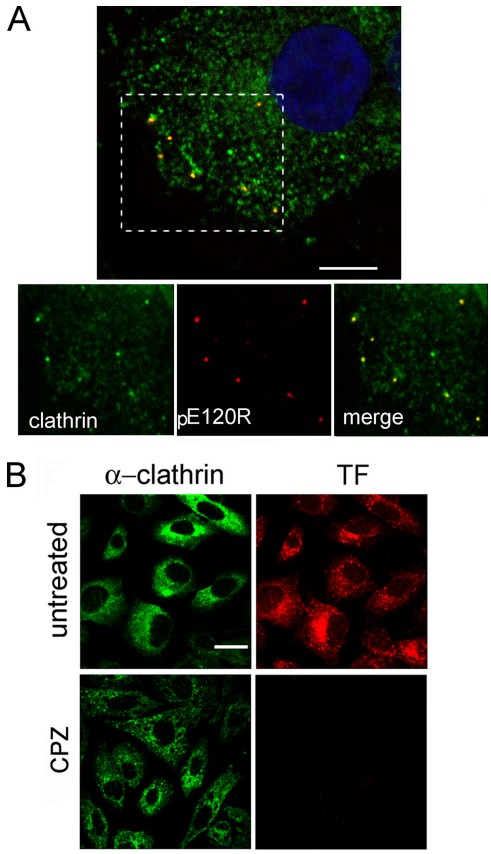

FIG. 3. Colocalization of ASFV with clathrin by confocal microscopy. (A) Vero cells infected with BA71V (>10 PFU/cell) and fixed at 0 to 20 min after adsorption were incubated with anti-ASFV structural protein pE120R (red) and anti-clathrin heavy chain (green) antibodies, followed by anti-rabbit IgG and anti-mouse IgG conjugated to A594 and A488, respectively. Colocalization of virions with clathrin can be observed in the representative 0.1-μm optical section at 5 min postinfection with nuclear staining TOPRO3 (blue). Bar, 15 μm. (B) Chlorpromazine inhibition of endocytosis. Vero cells were examined by confocal microscopy for TF-A_{594} uptake after treatment with different chlorpromazine (CPZ) concentrations. Only chlorpromazine at 14 μM is shown. The clathrin distribution was analyzed with a specific monoclonal antibody followed by anti-mouse conjugated to Alexa 488. Bar, 20 μm.

through clathrin-coated pits (CCPs). Benmerah et al. (7) demonstrated that deletion of Eps15 homology (EH) domains in Eps15 resulted in a dominant negative mutant of the protein (Eps15EΔ95/295) that arrested the formation of CCPs. Vero cells were first transfected with plasmids encoding either the mutant protein fused to GFP or the wild-type Eps15 form fused to GFP, and then transfected cells were assayed in a labeled TF uptake assay to verify the efficacy of the Eps15 dominant negative mutant. Figure 5A shows that transient overexpression of Eps15EΔ95/295, but not the wild type, effectively inhibited the internalization of TF, demonstrating that this dominant negative mutant is effective in Vero cells.

We next infected cells, at 24 h after transfection with these plasmids, with BA71V (MOI = 1 PFU/cell) and detected infected cells at 6 hpi by immunofluorescence with a specific anti-p30 monoclonal antibody and confocal microscopy. Transfected single cells were classified as infected or not infected according to p30 staining. The results showed numerous examples of cells expressing Eps15 fused to GFP and simultaneously positive for p30 staining, while expression of the dominant negative mutant fused to GFP predominantly excluded ASFV infection (Fig. 5B). Quantitation by counting multiple fields (more than 100 transfected cells in each case) revealed a significant reduction in the percentage of infected cells for cells expressing the dominant negative mutant Eps15EΔ95/295 compared to cells expressing wild-type Eps15 or GFP only as controls (Fig. 5C).

Taken together, the coincident results obtained with chlorpromazine treatment and dominant negative mutant proteins

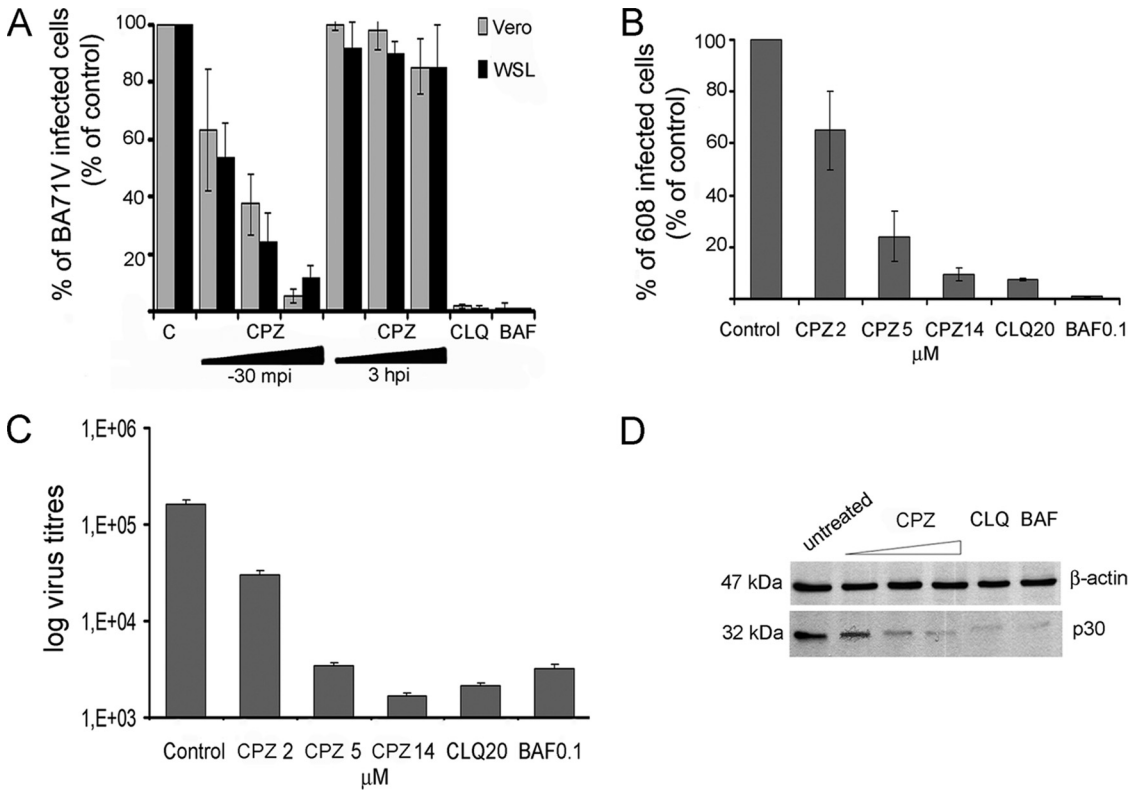

FIG. 4. CPZ inhibition of ASFV infection. (A and B) After CPZ treatment, Vero and WSL cells were infected with strain BA71V (A) or 608 VR13 (B), and infected cells were detected by FACS at 6 hpi, after staining with monoclonal anti-p30 antibody. The drug was added 30 min before infection or after 3 h of infection when indicated. Percentages relative to total infected cells found in controls are shown. The lysosomotropic agents chloroquine (CLQ) and bafilomycin A1 (BAF) were included as controls of infection inhibition. Error bars indicate standard deviations. (C) Effect of chlorpromazine on ASFV yields. Vero cells were incubated with different concentrations of chlorpromazine (CPZ) and then infected with BA71V (MOI, <1 PFU/cell). At 36 hpi, cells and media were harvested and virus titers analyzed by plaque assay (see Materials and Methods). (D) Inhibition of viral protein synthesis was analyzed by Western blotting of infected cells extracts with monoclonal anti-ASFV protein p30 at 6 hpi. Increasing concentrations of CPZ were used, and β-actin was detected as control of protein loading. In both cases, chloroquine (CLQ) and bafilomycin A1 (BAF) were included as controls.

support the hypothesis that ASFV entry is clathrin dependent and that the Eps15 component is required for a productive ASFV infection in Vero and WSL cells.

Role of cholesterol and caveolae in ASFV endocytosis. Previous studies (8) showed that the presence of cholesterol in cellular membranes is required for ASFV infection during early stages. Cholesterol is one of the main components of lipid raft microdomains, which are closely related to caveola formation. To analyze a possible role for caveolae during ASFV uptake, we examined the effect on ASFV infection of two different drug treatments that interfere with the caveola internalization pathway: nystatin and methyl-β-cyclodextrin (CD). Nystatin, a cholesterol-sequestering drug, disrupts membrane lipid rafts and consequently prevents caveola formation. On the other hand, the main effect of methyl-β-cyclodextrin is removal of cholesterol from plasma membranes. We first analyzed the cellular uptake of cholera toxin (CTX), which is generally used as a marker for caveolar endocytosis, in nystatin- and CD-treated Vero cells to check the effectiveness of the inhibitors at the concentrations used. As can be seen in Fig. 6A, labeled CTX internalization was almost completely inhibited by treatment with 25 to 50 μM nystatin and with 7 to 10 mM CD. Early studies (35, 41) demonstrated that depletion of cholesterol from the plasma membrane with CD also affected clathrin-mediated endocytosis, because cholesterol is essential for the formation of clathrin-coated vesicles. To evaluate this possibility, we examined TF uptake under these conditions. As expected, TF uptake was affected by CD treatment but not by nystatin (data not shown). Cholesterol levels in treated cell cultures were then measured, confirming a dose-dependent cholesterol depletion after CD treatment, while no significant differences in cholesterol content were found after nystatin and chlorpromazine treatment compared to control cells (Fig. 6B).

We analyzed the effect of these treatments on ASFV infection. Cholesterol reorganization at the plasma membrane induced by nystatin had no effect on ASFV infection, since no significant differences in infectivity, virus production, or p30 expression were observed compared to those for untreated infected cells. Nevertheless, cholesterol depletion by CD resulted in a clear and dose-dependent reduction in the percentages of Vero and WSL infected cells with the BA71V or 608VR13 isolates. As expected, this reduction correlated with a decrease in p30 expression levels, as judged by Western blot analysis, and also with a strong reduction in virus production (Fig. 6B to D and data not shown). Taken together, these results support the hypothesis that the requirement of choles-

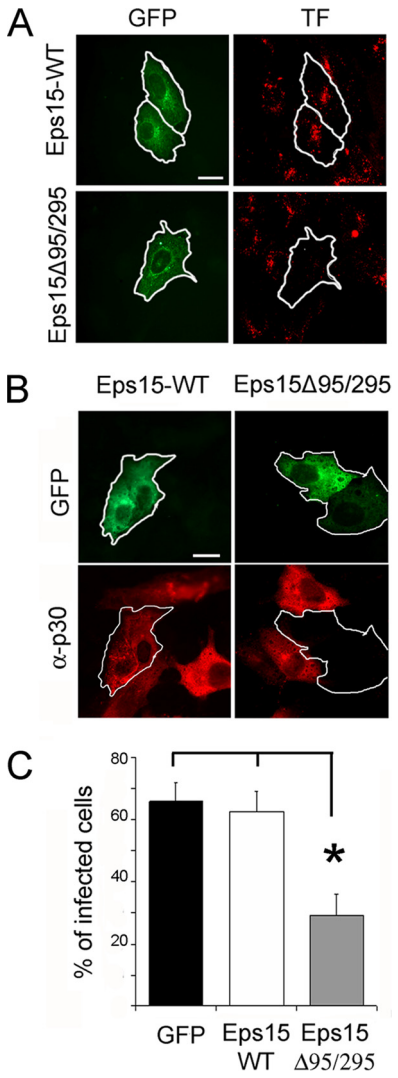

FIG. 5. Inhibition of ASFV entry by dominant negative mutant protein Eps15. Vero cells were transfected with plasmids encoding either wild-type Eps15-GFP or dominant negative mutant Eps15Δ95/295-GFP. (A) Transfected cells were examined by confocal microscopy for TF-A_{594} uptake to test the effectiveness of Eps15Δ95/295 for inhibition of clathrin-mediated endocytosis. (B) At 24 h after transfection, cells were infected with BA71V (MOI = 1 PFU/cell), and infected cells were detected at 6 hpi by immunofluorescence using anti-p30 monoclonal antibody followed by anti-mouse conjugated to Alexa 594 as a secondary antibody. Bar, 20 μm. (C) The numbers of transfected and simultaneously infected cells are expressed as percentages of viral antigen-positive cells. The means and standard deviations shown correspond to three experiments (>100 cells in each case).

terol in the plasma membrane for ASFV infection is more likely related to CCP formation than to lipid rafts/caveolae.

Effect of ion channel inhibitors and actin dynamic inhibition on ASFV infection. Recently, some studies have demonstrated that some viruses can use macropinocytosis to enter the endocytic pathway for a productive infection (reviewed in reference 30). We therefore decided to explore a potential role for macropinocytosis during ASFV infection using inhibitors of the Na^+/H^+ ion channels (amiloride and EIPA). To test the efficacy of these inhibitors, Vero cells treated with increasing inhibitor concentrations were tested for labeled dextran uptake. We observed by confocal microscopy that dextran internalization decreased from 25 μM EIPA and was almost completely abolished at 50 μM (Fig. 7A). Higher EIPA concentrations resulted in cell detachment. Amiloride, at concentrations that did not affect cell viability, did not prevent dextran uptake in Vero cells. Pretreatment of cells with EIPA affected ASFV infection, reducing the proportion of infected cells. Nevertheless, levels of viral protein p30 detected in infected cells extract at 6 hpi were not significantly modified after 25 μM EIPA treatment compared to those in control cells. A 25% reduction in p30 levels was found after 50 μM EIPA treatment, but we also observed cell detachment and high mortality (Fig. 7B).

Since actin plays a major role during macropinocytosis, we analyzed the effect of actin disruption in cells by use of jasplakinolide and latrunculin A. Addition of these inhibitors at 0.1 to 0.2 μM prior to infection did not affect the percentages of ASFV-infected cells detected by FACS (Fig. 7C).

DISCUSSION

Enveloped viruses can enter cells by direct fusion to membranes at the cell surface or can hijack endocytic pathways to infect host cells. Sensitivity to lysosomotropic agents has often been considered good evidence for endocytosis. This is the case for African swine fever virus infection, which was affected by these drugs, indicating that virus enters the cytoplasm of the host cell by receptor-mediated endocytosis rather than by direct fusion of viral envelope with the plasma membrane and also requires an acidification step. To discern which endocytosis pathway is required during the initial steps of ASFV infection to result in a productive infection, we used a variety of chemical inhibitors and molecular inhibitors in the form of dominant negative molecules.

We first examined the role of dynamin GTPase, which mediates membrane fission required for clathrin-mediated and lipid raft/caveola-based endocytosis (20). Two complementary approaches were used to disrupt dynamin-dependent endocytosis: use of dominant negative mutant K44A (14) and of dynasore, a specific and widely used chemical inhibitor of dynamin GTPase activity (1, 23–25). Transient expression of the K44A mutant significantly inhibited transferrin uptake and ASFV infection (about 50%) compared to wild-type dynamin or GFP alone. Infection was also dramatically inhibited by dynasore, in a dose-dependent manner. Even though the assays are different, both led to similar conclusions, indicating that ASFV entry into cells is dynamin dependent. This restricts the search to the dynamin-dependent routes of entry by endocytosis.

The involvement of dynamin and the low-pH dependence in ASFV infection (2, 44) suggest that clathrin-mediated endocytosis is the pathway for ASFV entry into Vero cells. Colocalization of ASFV virions with clathrin, detected by confocal microscopy during the first stages of infection, and reduction of infection in a dose-dependent manner after chlorpromazine, as well as chloroquine and bafilomycin, treatment prior to infection support this hypothesis. This confirms preliminary observations by EM (2) in which ASFV virions were often found adsorbed to cytoplasmic invaginations similar to clathrin-

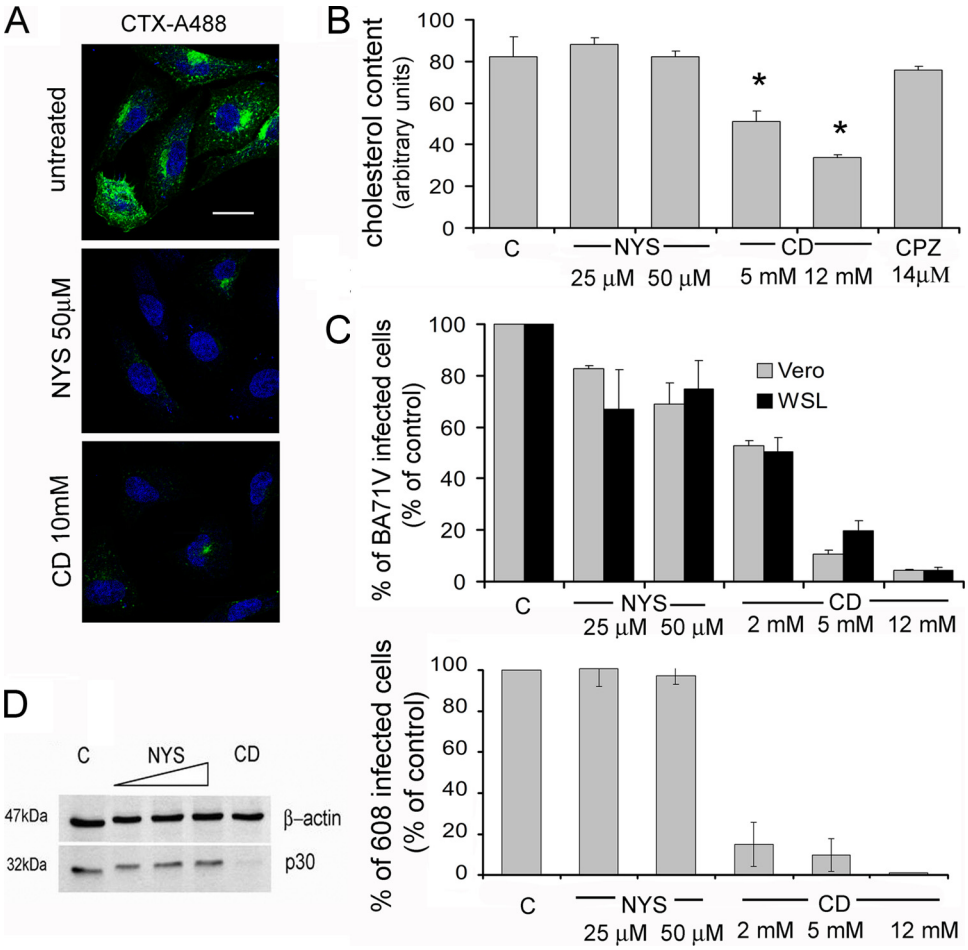

FIG. 6. Cholesterol is required during early stages of ASFV infection. (A) Internalization of cholera toxin (CTX) conjugated to Alexa 488 was examined by confocal microscopy in Vero cells previously treated with methyl-β-cyclodextrin (CD) and nystatin (NYS). Bar, 20 μm. (B) Cholesterol levels in cell extracts were determined after treatment with the different drugs used in the study. (C) The effects of cholesterol reorganization (NYS) and cholesterol depletion (CD) on ASFV infection are shown as percentages of infected cells at 6 hpi determined by FACS, normalized to total numbers of infected cells in untreated cultures. Infections with the BA71V isolate in Vero and WSL cells were compared after CD and NYS treatments (upper graph). Likewise, infection with 608VR13 isolate in Vero cells was analyzed after CD and NYS treatments (lower graph). The means and standard deviations shown correspond to three independent experiments. (D) Effects of NYS and CD on viral protein synthesis at 6 hpi were determined by Western blotting with specific antibodies.

coated pits but not in clathrin-coated vesicles. Nevertheless, chlorpromazine addition at 3 hpi, when most of the virions were already internalized, did not result in inhibition of ASFV infection, indicating that the correct assembly of clathrin is required specifically for ASFV internalization into host cells. However, these results do not exclude the possibility that clathrin may also be involved in some step of infection after 6 hpi. Indeed, it has been previously reported that ASFV infection at later times, during virus morphogenesis and assembly, affects the integrity of some component of the secretory pathway, such as the *trans*-Golgi network or clathrin adapter protein AP1 (28).

In order to examine more precisely the role of clathrin-mediated endocytosis in ASFV entry, we used an Eps15 dominant negative mutant fused to GFP (7, 40) to disrupt this endocytic pathway. Additionally, entry of mouse hepatitis virus type 2 has been recently shown to be a clathrin-dependent but Eps15-independent process (32). We demonstrated that transient expression of the Eps15 dominant negative mutant in Vero cells inhibited TF uptake and also markedly decreased the ability of ASFV to infect the transfected cells, thus confirming the importance of clathrin-mediated endocytosis and the essential component of the clathrin pathway Eps15 in ASFV infection. Convergent functional assays analyzing the dynamin- and clathrin-mediated endocytosis pathway by different means provided coincident results for ASFV infectivity inhibition.

Many other viruses from diverse families exploit clathrin-mediated endocytosis as the main or an accessory entry route (reviewed in references 15, 26, 27, and 31). Traditionally, cellular uptake by clathrin-mediated endocytosis was thought to be restricted to small ligands with a particle size limit of about 200 nm (34), which is precisely the diameter determined for extracellular ASFV enveloped virions (10). However, in recent studies clathrin and dynamin have been found to facilitate the entry of diverse zippering bacteria (48) that are larger than

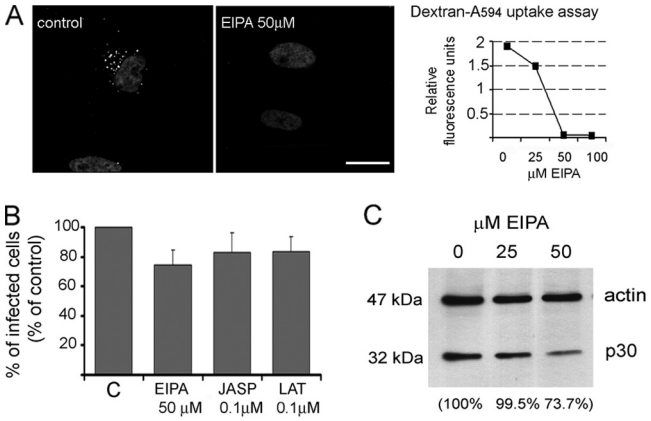

FIG. 7. Effect of ion channel blockers and actin polymerization inhibitors on ASFV infection. (A) To monitor the effectiveness of ion channel inhibitor EIPA, Vero cells were treated with different concentrations and examined for dextran-Alexa 594 uptake using confocal microscopy. Internalized dextran in control cells can be seen as a punctate staining close to the nucleus. Bar, 20 μm. Quantification of internalized dextran after EIPA treatment is also shown. (B) The number of infected cells at 6 hpi was scored by FACS after EIPA, jasplakinolide, and latrunculin A treatment. Error bars indicate standard deviations. (C) Cells were infected after EIPA treatment, and expression of early viral protein p30 was determined by Western blotting at 6 hpi.

ASFV virions, such as *Listeria* (46, 47) or *Chlamydia trachomatis* in nonphagocytic cells (23).

It has been previously shown that cholesterol in cellular membranes is relevant during the first stages of ASFV infection (8), and since cholesterol is involved in the lipid raft/caveola endocytosis pathway, we compared ASFV infectivities in cholesterol-depleted cells previously treated with methyl-β-cyclodextrin (CD) and subjected to cholesterol disorganization by treatment with nystatin, a sterol-binding drug that did not reduce the cholesterol levels. Our results are in concordance with previous observations showing that ASFV infection is sensitive to cholesterol depletion, while nystatin did not have any apparent effect. These results indicate that ASFV entry is a cholesterol-dependent process, because it is probably required to induce curvature in the plasma membrane in order to generate clathrin-coated pits and vesicles, as has been hypothesized previously (35, 41).

The induction of macropinocytosis to facilitate the entry of virus particles into host cells has been recently observed during vaccinia virus (29), adenovirus serotype 3 (5), and Kaposi's sarcoma-associated herpesvirus (18, 33) infection. Our preliminary studies using Na^+/H^+ ion channel and actin polymerization inhibitors suggest that macropinocytosis is not a constitutive pathway used by ASFV to enter the cell lines studied. Thus, the observed decrease in p30 levels after 50 μM EIPA treatment is likely to be due to adverse and unspecific effects induced by EIPA, as deduced by the cell detachment observed at this inhibitor concentration.

In summary, we have analyzed ASFV entry into host cells by disrupting diverse endocytic pathways with chemical inhibitors and also with specific dominant negative mutants to confirm previous observations and have identified those cellular factors that mediate ASFV uptake. We conclude that dynamin-dependent, clathrin-mediated uptake leads to productive entry by ASFV.

ACKNOWLEDGMENTS

We thank A. Dautry-Varsat for the kind gift of Eps15 plasmid constructs and S. Schmid for dynamin fused to GFP-coding vectors. We also especially thank Günther Keil for the WSL-R cell line.

This work was supported by Plan Nacional grants CSD2006-00007, PET2006-0785, and AGL2009-09209 from the Ministerio de Ciencia e Innovacion; by Wellcome Trust grant WT075813; and by EU grant EPIZONE FOOD-CT2006-016236.

REFERENCES

1. **Abban, C. Y., N. A. Bradbury, and P. I. Meneses.** 2008. HPV16 and BPV1 infection can be blocked by the dynamin inhibitor dynasore. Am. J. Ther. **15:**304–311.
2. **Alcami, A., A. L. Carrascosa, and E. Vinuela.** 1989. The entry of African swine fever virus into Vero cells. Virology **171:**68–75.
3. **Alfonso, P., J. Rivera, B. Hernaez, C. Alonso, and J. M. Escribano.** 2004. Identification of cellular proteins modified in response to African swine fever virus infection by proteomics. Proteomics **4:**2037–2046.
4. **Alonso, C., J. Miskin, B. Hernaez, P. Fernandez-Zapatero, L. Soto, C. Canto, I. Rodriguez-Crespo, L. Dixon, and J. M. Escribano.** 2001. African swine fever virus protein p54 interacts with the microtubular motor complex through direct binding to light-chain dynein. J. Virol. **75:**9819–9827.
5. **Amstutz, B., M. Gastaldelli, S. Kalin, N. Imelli, K. Boucke, E. Wandeler, J. Mercer, S. Hemmi, and U. F. Greber.** 2008. Subversion of CtBP1-controlled macropinocytosis by human adenovirus serotype 3. EMBO J. **27:**956–969.
6. **Angulo, A., A. Alcami, and E. Vinuela.** 1993. Virus-host interactions in African swine fever: the attachment to cellular receptors. Arch. Virol. Suppl. **7:**169–183.
7. **Benmerah, A., M. Bayrou, N. Cerf-Bensussan, and A. Dautry-Varsat.** 1999. Inhibition of clathrin-coated pit assembly by an Eps15 mutant. J. Cell Sci. **112:**1303–1311.
8. **Bernardes, C., A. Antonio, M. C. Pedroso de Lima, and M. L. Valdeira.** 1998. Cholesterol affects African swine fever virus infection. Biochim. Biophys. Acta **1393:**19–25.
9. **Brodsky, F. M., C. Y. Chen, C. Knuehl, M. C. Towler, and D. E. Wakeham.** 2001. Biological basket weaving: formation and function of clathrin-coated vesicles. Annu. Rev. Cell Dev. Biol. **17:**517–568.
10. **Carrascosa, J. L., J. M. Carazo, A. L. Carrascosa, N. Garcia, A. Santisteban, and E. Vinuela.** 1984. General morphology and capsid fine structure of African swine fever virus particles. Virology **132:**160–172.
11. **Chu, J. J., and M. L. Ng.** 2004. Infectious entry of West Nile virus occurs through a clathrin-mediated endocytic pathway. J. Virol. **78:**10543–10555.
12. **Daecke, J., O. T. Fackler, M. T. Dittmar, and H. G. Krausslich.** 2005. Involvement of clathrin-mediated endocytosis in human immunodeficiency virus type 1 entry. J. Virol. **79:**1581–1594.
13. **Damke, H., T. Baba, A. M. van der Bliek, and S. L. Schmid.** 1995. Clathrin-independent pinocytosis is induced in cells overexpressing a temperature-sensitive mutant of dynamin. J. Cell Biol. **131:**69–80.
14. **Damke, H., T. Baba, D. E. Warnock, and S. L. Schmid.** 1994. Induction of mutant dynamin specifically blocks endocytic coated vesicle formation. J. Cell Biol. **127:**915–934.
15. **DeTulleo, L., and T. Kirchhausen.** 1998. The clathrin endocytic pathway in viral infection. EMBO J. **17:**4585–4593.
16. **Dixon, L., J. V. Costa, J. M. Escribano, D. L. Rock, E. Vinuela, and P. J. Wilkinson (ed.).** 2000. Asfarviridae. Academic Press, New York, NY.
17. **Gomez-Puertas, P., F. Rodriguez, J. M. Oviedo, A. Brun, C. Alonso, and J. M. Escribano.** 1998. The African swine fever virus proteins p54 and p30 are involved in two distinct steps of virus attachment and both contribute to the antibody-mediated protective immune response. Virology **243:**461–471.
18. **Greene, W., and S. J. Gao.** 2009. Actin dynamics regulate multiple endosomal steps during Kaposi's sarcoma-associated herpesvirus entry and trafficking in endothelial cells. PLoS Pathog. **5:**e1000512.
19. **Helenius, A., J. Kartenbeck, K. Simons, and E. Fries.** 1980. On the entry of Semliki forest virus into BHK-21 cells. J. Cell Biol. **84:**404–420.
20. **Henley, J. R., E. W. Krueger, B. J. Oswald, and M. A. McNiven.** 1998. Dynamin-mediated internalization of caveolae. J. Cell Biol. **141:**85–99.
21. **Hernaez, B., J. M. Escribano, and C. Alonso.** 2008. African swine fever virus protein p30 interaction with heterogeneous nuclear ribonucleoprotein K (hnRNP-K) during infection. FEBS Lett. **582:**3275–3280.
22. **Hernaez, B., J. M. Escribano, and C. Alonso.** 2006. Visualization of the African swine fever virus infection in living cells by incorporation into the virus particle of green fluorescent protein-p54 membrane protein chimera. Virology **350:**1–14.
23. **Hybiske, K., and R. S. Stephens.** 2007. Mechanisms of Chlamydia trachomatis entry into nonphagocytic cells. Infect. Immun. **75:**3925–3934.
24. **Kirchhausen, T., E. Macia, and H. E. Pelish.** 2008. Use of dynasore, the

small molecule inhibitor of dynamin, in the regulation of endocytosis. Methods Enzymol. **438:**77–93.
25. **Macia, E., M. Ehrlich, R. Massol, E. Boucrot, C. Brunner, and T. Kirchhausen.** 2006. Dynasore, a cell-permeable inhibitor of dynamin. Dev. Cell **10:**839–850.
26. **Marsh, M., and A. Helenius.** 2006. Virus entry: open sesame. Cell **124:**729–740.
27. **Marsh, M., and A. Pelchen-Matthews.** 2000. Endocytosis in viral replication. Traffic **1:**525–532.
28. **McCrossan, M., M. Windsor, S. Ponnambalam, J. Armstrong, and T. Wileman.** 2001. The trans Golgi network is lost from cells infected with African swine fever virus. J. Virol. **75:**11755–11765.
29. **Mercer, J., and A. Helenius.** 2008. Vaccinia virus uses macropinocytosis and apoptotic mimicry to enter host cells. Science **320:**531–535.
30. **Mercer, J., and A. Helenius.** 2009. Virus entry by macropinocytosis. Nat. Cell Biol. **11:**510–520.
31. **Pelkmans, L., and A. Helenius.** 2003. Insider information: what viruses tell us about endocytosis. Curr. Opin. Cell Biol. **15:**414–422.
32. **Pu, Y., and X. Zhang.** 2008. Mouse hepatitis virus type 2 enters cells through a clathrin-mediated endocytic pathway independent of Eps15. J. Virol. **82:**8112–8123.
33. **Raghu, H., N. Sharma-Walia, M. V. Veettil, S. Sadagopan, and B. Chandran.** 2009. Kaposi's sarcoma-associated herpesvirus utilizes an actin polymerization-dependent macropinocytic pathway to enter human dermal microvascular endothelial and human umbilical vein endothelial cells. J. Virol. **83:**4895–4911.
34. **Rejman, J., V. Oberle, I. S. Zuhorn, and D. Hoekstra.** 2004. Size-dependent internalization of particles via the pathways of clathrin- and caveolae-mediated endocytosis. Biochem. J. **377:**159–169.
35. **Rodal, S. K., G. Skretting, O. Garred, F. Vilhardt, B. van Deurs, and K. Sandvig.** 1999. Extraction of cholesterol with methyl-beta-cyclodextrin perturbs formation of clathrin-coated endocytic vesicles. Mol. Biol. Cell **10:**961–974.
36. **Sanchez-Torres, C., P. Gomez-Puertas, M. Gomez-del-Moral, F. Alonso, J. M. Escribano, A. Ezquerra, and J. Dominguez.** 2003. Expression of porcine CD163 on monocytes/macrophages correlates with permissiveness to African swine fever infection. Arch. Virol. **148:**2307–2323.
37. **Sever, S., H. Damke, and S. L. Schmid.** 2000. Dynamin:GTP controls the formation of constricted coated pits, the rate limiting step in clathrin-mediated endocytosis. J. Cell Biol. **150:**1137–1148.
38. **Sieczkarski, S. B., and G. R. Whittaker.** 2002. Dissecting virus entry via endocytosis. J. Gen. Virol. **83:**1535–1545.
39. **Sieczkarski, S. B., and G. R. Whittaker.** 2002. Influenza virus can enter and infect cells in the absence of clathrin-mediated endocytosis. J. Virol. **76:**10455–10464.
40. **Stuart, A. D., and T. D. Brown.** 2006. Entry of feline calicivirus is dependent on clathrin-mediated endocytosis and acidification in endosomes. J. Virol. **80:**7500–7509.
41. **Subtil, A., I. Gaidarov, K. Kobylarz, M. A. Lampson, J. H. Keen, and T. E. McGraw.** 1999. Acute cholesterol depletion inhibits clathrin-coated pit budding. Proc. Natl. Acad. Sci. U. S. A. **96:**6775–6780.
42. **Sun, X., V. K. Yau, B. J. Briggs, and G. R. Whittaker.** 2005. Role of clathrin-mediated endocytosis during vesicular stomatitis virus entry into host cells. Virology **338:**53–60.
43. **Tulman, E. R., G. A. Delhon, B. K. Ku, and D. L. Rock.** 2009. African swine fever virus. Curr. Top. Microbiol. Immunol. **328:**43–87.
44. **Valdeira, M. L., C. Bernardes, B. Cruz, and A. Geraldes.** 1998. Entry of African swine fever virus into Vero cells and uncoating. Vet. Microbiol. **60:**131–140.
45. **Valdeira, M. L., and A. Geraldes.** 1985. Morphological study on the entry of African swine fever virus into cells. Biol. Cell **55:**35–40.
46. **Veiga, E., and P. Cossart.** 2005. Listeria hijacks the clathrin-dependent endocytic machinery to invade mammalian cells. Nat. Cell Biol. **7:**894–900.
47. **Veiga, E., and P. Cossart.** 2006. The role of clathrin-dependent endocytosis in bacterial internalization. Trends Cell Biol. **16:**499–504.
48. **Veiga, E., J. A. Guttman, M. Bonazzi, E. Boucrot, A. Toledo-Arana, A. E. Lin, J. Enninga, J. Pizarro-Cerda, B. B. Finlay, T. Kirchhausen, and P. Cossart.** 2007. Invasive and adherent bacterial pathogens co-opt host clathrin for infection. Cell Host Microbe **2:**340–351.